https://doi.org/10.5194/egusphere-2026-7065
Preprint. Discussion started: 26 November 2026
© Author(s) 2026. CC BY 4.0 License.

Seaweed and coastal plant biomass-stimulated methane emissions driven by methylated compound content

Ning Hall[1,2], Hanif Prayitno[1], Jon Bumbak[1], Leith Murray[1], Sophie Golding-Chan[1], Riley Herron[3], Wei Wen Wong[1], Katherine J. Jeppe[4], Christopher K. Barlow[4], Chris Greening[2], and Perran L. M. Cook[1]

[1]Water Studies, School of Chemistry, Monash University, Melbourne, 3800, Australia
[2]CLIMB Research Unit, Biomedicine Discovery Institute, Department of Microbiology, Monash University, Melbourne, 3800, Australia
[3]Australian Centre for Research on Separation Science, School of Chemistry, Monash University, Melbourne, Australia
[4]Monash Proteomics and Metabolomics Platform, Department of Biochemistry and Molecular Biology, Biomedicine Discovery Institute, Monash University, Melbourne, 3800, Australia

Correspondence to: Ning Hall (ninghall0@gmail.com) and Perran L. M. Cook (perran.cook@monash.edu)

Abstract. Methane emissions from coastal sediments are increasingly influenced by ecological change, including eutrophication-driven seaweed blooms and efforts to restore coastal vegetation. Yet the pathways and variability of methane production in these daenvironments remain poorly constrained. Here, we compared methane production from three seaweeds (Ulva, red filamentous algae, and kelp) and three coastal plants (mangrove leaves, saltmarsh plants, and seagrass) in sands from Port Phillip Bay, Australia. To identify potential predictive precursors, we quantified key methylated osmolytes (dimethyl sulfoniopropionate (DMSP), choline, trimethylamine (TMA), trimethylamine N-oxide (TMAO)), that serve as methanogenic substrates. Methane production from seaweeds was strongly correlated with osmolyte content, whereas mangrove leaves stimulated the highest methane production even though measured osmolytes could account for less than 10% of it. Methanol was not detected in fresh mangrove leaves but accumulated during their degradation in sediment slurries. In separate incubations of four Port Phillip Bay sediments, pectin additions produced a transient methanol pulse, and high-methoxyl pectin stimulated 6- to 32-fold more methane than low-methoxyl pectin in three of the four sediments, whereas methanol added directly was largely consumed without conversion to methane (< 8% of the theoretical yield). Methyl-esterified plant polymers are therefore a candidate methane source in coastal sediments, but the pathway linking them to methanogenesis, and their contribution to methane production from mangrove leaves, remain to be established. These findings broaden the understanding of organic matter sources fuelling methanogenesis in coastal sediments and highlight an overlooked contribution of both seaweeds and plants to coastal methane cycling.

1 Introduction

Coastal waters represent the largest and most uncertain component of global marine methane (CH_4) emissions, generating up to ~75% of total marine fluxes despite occupying only ~15% of the ocean surface area (Weber et al., 2019; Borges et al., 2016; Rosentreter et al., 2021). Methane supersaturation in these environments is driven by multiple processes, including submarine groundwater discharge (Cable et al., 1996; Kim and Hwang, 2002), riverine

https://doi.org/10.5194/egusphere-2026-7065
Preprint. Discussion started: 26 November 2026
© Author(s) 2026. CC BY 4.0 License.

and estuarine inputs (Bussmann et al., 2021), and *in situ* production within vegetated habitats such as seagrass beds, salt marshes, and mangroves (Al-Haj and Fulweiler, 2020).

In coastal sediments, methylotrophic methanogenesis has emerged as a dominant methane-producing pathway, particularly in habitats receiving inputs from seaweeds and coastal vegetation (Xiao et al., 2018; Tsola et al., 2021; Schorn et al., 2022; Roth et al., 2023; Hall et al., 2025; Zhuang, 2026). In high-sulfate marine waters, sulfate-reducing bacteria outcompete acetoclastic and hydrogenotrophic methanogens for acetate and hydrogen; however, methylotrophic methanogens bypass this competitive inhibition by utilizing non-competitive methylated substrates (Oremland et al, 1982a, b). These substrates—primarily methylamines, methylsulfides, and osmolytes such as glycine betaine, choline, trimethylamine N-oxide (TMAO) and dimethylsulfoniopropionate (DMSP)—are synthesized in high concentrations by macroalgae and coastal plants to mitigate osmotic stress (Burg and Ferraris, 2008; Yoch, 2002). Upon cellular breakdown, these osmolytes enter the sediment microbial pool (Wang and Lee, 1994; Oren, 1988). Additionally, the decomposition of plant cell walls can release methanol through the demethylation of pectin, potentially providing a further substrate for methylotrophs (Fall and Benson, 1996; Wang et al., 2021). Due to the shallow depths and turbulent hydrodynamics characteristic of coastal zones, a substantial fraction (approx. 50%) of this sediment-produced methane may evade microbial oxidation and is rapidly transported into the water column and ultimately the atmosphere via advection, ebullition, and diffusion (Santos et al., 2012; Mao et al., 2022).

Despite the established link between methylated plant compounds and methane production, a critical knowledge gap remains: the specific methanogenic potential and methylated chemical composition of different seaweed and coastal plant species are largely uncharacterized. Addressing this gap is increasingly urgent as climate change and eutrophication rapidly restructure coastal vegetation. Seaweed aquaculture is expanding at ~6% annually (Duarte et al., 2022) and is now recognized as a potential methane source (Deng et al., 2026). Simultaneously, ocean warming and eutrophication are accelerating macro- and microalgal blooms, notably of *Ulva* species (Green-Gavrielidis and Thornber, 2022; Qi et al., 2025), while restoration initiatives are expanding mangroves, salt marshes, and seagrasses (Buelow et al., 2022; Wang et al., 2022). Conversely, marine heatwaves and warming oceans are causing widespread declines in kelp forest cover (Smale, 2020). Collectively, these shifts in vegetative composition will alter organic inputs and methane cycling in shallow coastal ecosystems. Without a mechanistic understanding of how different plant and macroalgal biomasses stimulate methane production, predicting the magnitude and direction of future marine methane emissions remains highly uncertain.

To address this knowledge gap, we ask: (i) do seaweed and coastal plant inputs stimulate methane production to different extents, (ii) is methane production related to the tissue content of methylated osmolytes (DMSP, choline, TMA and TMAO) or to non-osmolyte organic matter, and (iii) can methyl-esterified pectin, a potential source of methanol during plant decay, stimulate methane production in coastal sediments? Addressing these questions will improve understanding of how shifts in the quantity and composition of degrading coastal plants and seaweed

https://doi.org/10.5194/egusphere-2026-7065
Preprint. Discussion started: 26 November 2026
© Author(s) 2026. CC BY 4.0 License.

influence methane emissions in marine ecosystems being rapidly changed by climate change, eutrophication, and ecological restoration efforts (Trégarot et al., 2024).

2 Methods

2.1 Field sites and sampling

Five sandy beach sites around Port Phillip Bay, Victoria, Australia were chosen for sand and seaweed collection investigating interspecies variation in methane production (Fig. 1), which was undertaken on 2nd October 2023. The sites in the western portion of the bay (Werribee and Altona) are influenced by nitrogen emissions from the Western Treatment Plant, and have historically suffered from drift algal blooms, while the eastern sites experience lower nutrient loads (Wong et al., 2022; Valero-Rodriguez et al., 2024). Three dominant types of seaweed were collected (unattached only i.e. beach-cast, not still growing) from each site to represent algal condition when it begins to degrade. Sea lettuce (*Ulva lactuca*), and common kelp (*Ecklonia radiata*) were present at all sites. Red filamentous algae (*Ceramiales*) were collected at all sites, with *Ceramiaceaen "thamnions"* collected at Elwood (-37.8814, 144.9758), St Kilda (-37.8624, 144.9708) and Green Point (-37.9238, 144.9864) and *Rhodomelacean "polysiphonia"* collected at Altona (-37.8714, 144.8376) and Werribee (-37.9722, 144.7004). A second field trip was undertaken on 1st August 2024 to investigate the effect of seagrass, mangrove and salt marsh plants (collectively "coastal plants") on methane production. Samples of mangrove leaves (*Avicennia marina*, commonly white mangrove or grey mangrove) and saltmarsh plant (*Salicornia quinqueflora*, commonly beaded samphire) were collected from Hastings (-38.3138, 145.1958). Seagrass (*Amphibolis antarctica*, commonly wire weed or sea nymph) was collected from Flinders (-38.4808, 145.0270). All biomass samples were transported to the lab in a cold box and refrigerated until use (within 24-48 hours). Sand was collected with acrylic cores from the intertidal zone (Werribee 2nd October 2023 trip, Flinders, 1st August 2024 trip) and transported back to the lab where the surface 0–5 cm was sectioned, homogenised and sieved through a 1 mm mesh to remove shells and other large debris. Surface 0–5 cm depth was chosen as this is the sediment layer with the highest contact with beach-cast seaweed and coastal plant biomass and have previously been shown to host seed populations of rapidly growing oxygen tolerant methylotrophic methanogens such as Methanococcoides *sp*. (Hall et al., 2025). Properties of the Werribee sand are given in Table 1.

https://doi.org/10.5194/egusphere-2026-7065
Preprint. Discussion started: 26 November 2026
© Author(s) 2026. CC BY 4.0 License.

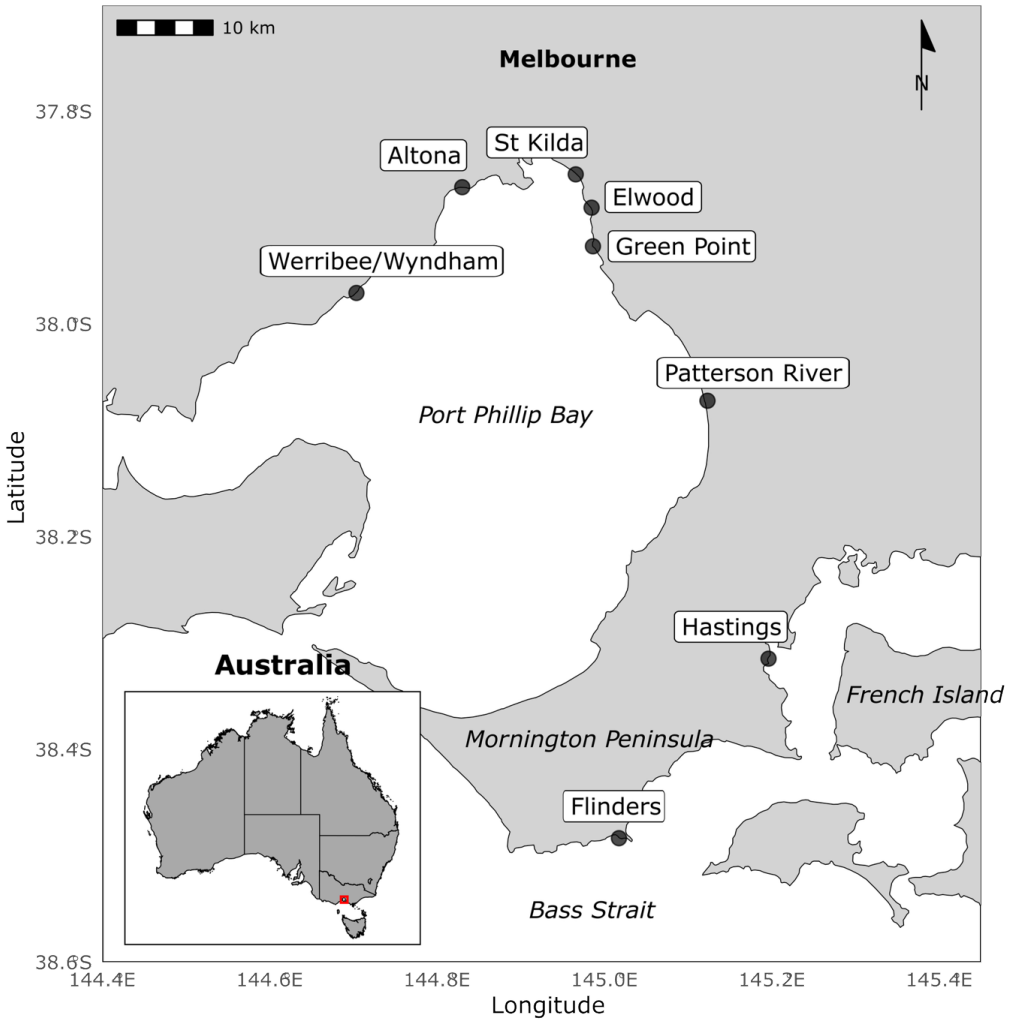


Figure 1. Map of field sites in the study. Basemap produced with data from Geoscience Australia (https://pid.geoscience.gov.au/service/ga/100194).

2.2 Preliminary pure-substrate slurry experiment

Sand slurries were prepared in triplicate with 30 g of sand and 70 mL of unfiltered seawater, collected from Werribee in September 2021, weighed into a 160 mL serum vial. Pure substrates dimethyl sulfide (DMS), methylamine, and glycine betaine were added to a final concentration of 100 µM. Slurries were crimp-capped with butyl rubber stoppers and the headspace purged with argon, shaken to equilibrium, and purged again (3 minutes each time) to create anoxic conditions. Incubations occurred under ambient laboratory conditions (approx. 20°C, ambient light). Headspace gas samples were taken at time 0, 13, 22, 41, 66, 85, and 110 h. At each time point, 2 mL of helium was injected into each

https://doi.org/10.5194/egusphere-2026-7065
Preprint. Discussion started: 26 November 2026
© Author(s) 2026. CC BY 4.0 License.

slurry to prevent under pressurisation, gently shaken, and a 2 mL headspace gas sample taken and injected into a helium-purged 3 mL exetainer (over pressurised).

2.3 Biomass incubation slurry experiments

Slurries were prepared and sampled as described above. For slurries with seaweed or plant addition, approximately 100 mg wet weight of roughly cut up tissue was added to the serum vial. Sub-samples were also taken and frozen at -20°C for metabolomic analysis. Headspace samples were taken at time 0, 50, 120, 220, 320, and 460 hours for seaweeds, and 0, 21, 72, 96, 120, 170, and 180 hours for coastal plants. For controls, sand slurries were prepared in duplicate, and either had no addition of biomass or were amended with DMS (80 µM) or TMA (100 µM final concentration). Methanol production during mangrove leaf degradation was examined in a separate experiment (Sect. 2.4), and methane and methanol production from pectin in sediments from four further sites (Sect. 2.5).

2.4 Methanol production during mangrove leaf degradation

Methanol production pathways in mangrove leaves were examined in the presence and absence of BES (2-bromoethane sulfonate, 30 mM, an inhibitor of methanogenesis), and 3 mM sodium molybdate (an inhibitor of sulfate reduction). Slurry incubations were prepared in triplicate using 20 mL serum vials. Experimental samples contained 500 mg (wet weight) of mangrove leaves (crushed with a mortar and pestle), 5 g of sand, and 10 mL of seawater. Two control groups were established: a sediment-only control (5 g sand and 10 mL seawater) and a leaf-only control (500 mg crushed leaves and 10 mL seawater).

The vials were capped with butyl rubber stoppers and purged as described above to create anoxic conditions. This experiment included a sediment only control, sediment + mangrove leaves, sediment + mangrove leaves plus the methanogenesis inhibitor sodium 2-bromoethanesulfonate (BES), sediment + mangrove leaves + BES + the sulfate reduction inhibitor molybdate (King et al, 1983). Samples of the water were taken for methanol analysis immediately, and after 144 hours (sampling time chosen to coincide with peak methane production in previous mangrove leaf slurries) and filtered (0.45 µm syringe filter) before analysis. Methane was not measured in these vials.

Differences in methanol concentration (nmol per mg leaf dry weight) between sample groups were assessed using a one-way analysis of variance (ANOVA), with pairwise comparisons conducted via Tukey's Honest Significant Difference (HSD) post-hoc test. All statistical analyses were performed in R (version 4.6.0), using the rstatix v. 0.7.3 package for hypothesis testing. Results were considered statistically significant at $p < 0.05$, using adjusted p-values from the Tukey HSD test.

2.5 Pectin and methanol amendment experiments

To test whether methyl-esterified plant polymers can stimulate methane production in coastal sediments, a separate set of slurry incubations was carried out with surface sediments from four further sites around Port Phillip Bay: a

https://doi.org/10.5194/egusphere-2026-7065
Preprint. Discussion started: 26 November 2026
© Author(s) 2026. CC BY 4.0 License.

sheltered sandy beach at St Kilda, a sandy site at Wyndham Harbour, and estuarine muds from the Patterson River and the Werribee South boat ramp (Figure 1). Sediments were sieved (1 mm) and homogenised, and 10 g of wet sediment was added to 160 mL serum vials together with 100 mL of site seawater containing one of five amendments: no addition (control), high-methoxyl (HM) pectin (0.05 g L^{-1}, i.e. 5 mg per vial), low-methoxyl (LM) pectin (0.05 g L^{-1}), methanol (nominally 100 µM) or glucose (1 mM). Both pectins were non-amidated, food-grade products manufactured in Germany (Melbourne Food Depot, Australia). Each treatment was prepared in triplicate. Vials were sealed with butyl rubber stoppers and aluminium crimp caps, and the headspace was purged with N_2 and returned to atmospheric pressure. Vials were incubated at room temperature (approx. 20 °C). Properties of the four sediments are given in Table 1.

Headspace and water samples (2 mL each) were taken at the start of the incubation and after 1, 2, 3, 4, 7, 11 and 21 days (St Kilda) or 3, 6, 9, 12 and 21 days (other sites). The headspace volume removed was replaced with N_2. Gas samples were transferred to evacuated 12.5 mL vials, brought to atmospheric pressure with N_2 and analysed for methane by gas chromatography (Sect. 2.6). Water samples were filtered (0.45 µm) and analysed for methanol by GC–FID as described in Sect. 2.7, with calibration standards of 0–1240 µM. Methanol was measured until day 7 (St Kilda) or day 12 (other sites). Methanol concentrations in the unamended controls (9–10 µM) were close to the concentration corresponding to zero peak area in the calibration (8.6 µM) and are therefore treated as background.

Total methane in each vial was calculated from the headspace mixing ratio, the headspace volume (approx. 55 mL, allowing for 100 mL of water and approx. 5 mL of sediment) and the dissolved methane in equilibrium with the headspace, calculated with the solubility of methane in seawater at 20 °C (Wiesenburg and Guinasso, 1979). Methane removed in earlier headspace samples was added back. Methane production was calculated relative to the initial value in each vial and normalised to the wet weight of sediment (nmol g^{-1}). To assess how efficiently each substrate was converted to methane, the maximum methane production in excess of the unamended control was compared with the theoretical yield of ¾ mol CH_4 per mol of methanol or methyl ester (Ferry, 1999) and 3 mol CH_4 per mol of glucose. The amount of methanol added was taken as the measured initial methanol concentration in the methanol treatment minus that in the controls. The supplier did not specify the methyl ester content of the pectins. We therefore estimated it from the degrees of esterification typical of commercial HM (55–75%) and LM (25–45%) pectins and a galacturonic acid content of 65–85% (May, 1990), giving 9.7–17.1 µmol and 4.5–10.5 µmol of methyl ester per vial for HM and LM pectin, respectively.

Table 1. Properties of the surface sediments (0–5 cm) used in the incubations. All sediments were collected from < 1 m water depth. C and N are given as a percentage of dry weight, and D_{50} is the median grain size. Grain size classes: clay < 3.9 µm, silt 3.9–63 µm, sand 63–2000 µm. –, not measured. [a]From Chen et al. (2022), site C.

Sediment	Location	Incubations	C (%)	N (%)	D_{50} (µm)	Clay (%)	Silt (%)	Sand (%)
Werribee sand (beach)	−37.9724, 144.7003	Seaweeds (Sect. 2.3)	0.23	0.05	165	0.7	6.9	92.4
St Kilda sand (beach, sheltered)	−37.8613, 144.9691	Pectin and methanol (Sect. 2.5)	–	–	217[a]	–	–	–

https://doi.org/10.5194/egusphere-2026-7065
Preprint. Discussion started: 26 November 2026
© Author(s) 2026. CC BY 4.0 License.

Patterson River mud (estuarine)	−38.0707, 145.1273	Pectin and methanol (Sect. 2.5)	1.64	0.17	101	9.0	36.0	55.0
Wyndham Harbour sand (beach)	−37.9638, 144.7108	Pectin and methanol (Sect. 2.5)	0.08	0.02	259	0.0	0.0	100.0
Werribee South mud (estuarine, cohesive)	−37.9723, 144.6859	Pectin and methanol (Sect. 2.5)	0.50	0.07	148	2.4	13.9	83.7

2.6 Methane analysis

Headspace methane concentration was monitored over time to determine methane production potential of the seaweeds and coastal plants. Samples were analysed by Gas chromatography–pulse discharge helium ionisation detection (GC–PDHID; Valco Instruments Co. Inc.). Manual triplicate five-point calibration was performed at the start of each run using NATA-accredited calibration gases from Air Liquide and BOC HiQ, along with standards and blanks every 20–30 samples to monitor for instrumental drift.

2.7 Methanol Analysis

Methanol analysis was conducted by GC–FID (PerkinElmer Inc.). The GC was fitted with a polar ZB-WaxPlus column (30 m × 0.32 mm internal diameter (ID) x 1.0 µm film thickness (d_f); Phenomenex, Inc.). The injector was operated in split mode (20:1 ratio) and heated to 120°C. Ultrahigh purity grade hydrogen (99.999%) was used as the carrier gas, with a constant flow rate of 1.5 mL min^{-1}. The initial oven temperature was set to 120°C and held for 3.5 min, for a total analysis time of 3.5 min. The FID temperature was set to 250°C. Samples were introduced via 1 µL manual injections of the water phase. Manual triplicate 5-point calibration was performed.

2.8 Metabolomics

For metabolomic analysis, frozen seaweed and plant samples were placed in 1.5 mL Eppendorf microtubes (kept frozen in dry ice) and crushed under liquid nitrogen with a stainless-steel pestle. A 20–50 mg sample of crushed seaweed was then weighed frozen and extraction solvent was added at 20 µL mg^{-1} tissue. The extraction solvent was 2:6:1 chloroform:methanol:water with 2 µM CHAPS, CAPS, PIPES and TRIS as internal standards for complex biological samples to monitor and correct for sample-to-sample differences in matrix effects caused by biomass components, differences in injection volume, and instrument response. Samples were then vortexed briefly, sonicated in an ice bath for 10 min, centrifuged at 20,000 g for 10 min at 4°C. The supernatant was then transferred to an LC-MS vial and analysed in triplicate by liquid-chromatography mass spectrometry (LC-MS). LC-MS was performed using a Vanquish Horizon coupled to a Q-Exactive Plus Orbitrap (Thermo Fisher Scientific, Australia). The chromatography used hydrophilic interaction liquid chromatography coupled to high-resolution mass spectrometry.

https://doi.org/10.5194/egusphere-2026-7065
Preprint. Discussion started: 26 November 2026
© Author(s) 2026. CC BY 4.0 License.

Chromatographic separation was achieved on a 5 µm 150 x 4.6 mm iHILIC®-(P) Classic (Hilicon, Sweden) column using with a 1290 Inline Filter, 0.3 µm (Agilent) guard column with a gradient elution of 20 mM ammonium carbonate (A) and acetonitrile (B) (linear gradient time-% B as follows: 0 min-80%, 15 min-50%, 18 min-5%, 21 min-5%, 24 min-80%, 32 min-80%) at 25°C. The flow rate was maintained at 500 µL min^{-1}. Samples were kept at 6°C in the autosampler and 10 µL was injected for analysis. Mass spectrometry was performed at 70,000 resolution operating in rapid switching positive (4 kV) and negative (−3.5 kV) mode electrospray ionization (capillary temperature 300°C; sheath gas flow rate 50; auxiliary gas flow rate 20; probe temp 120°C).

A seven-point calibration curve was used for quantification of TMA, TMAO, DMSP and choline, all reported concentrations fell within the calibration range (Table 2, samples below LOD were reported as 0). Peak integration of target metabolites was performed in Skyline 24.1. (Pino et al., 2020; MacLean et al., 2010; Skyline for Small Molecules, n.d.). We note metabolites were not measured during the incubations (either water or plant material) due to the logistical problem of taking plant material from the vial, analytical problems with high salinity and high sample analysis cost. Glycine betaine was not quantified as preliminary experiments showed that the addition of this compound to the sediment studied produced negligible methane compared to DMS and TMA (Fig. 2).

Table 2. LOD of analytes, calculated according to ICH Harmonised Tripartite Guideline (2005).

Compound	LOD (µM)
Choline	0.08
DMSP	1.51
TMA	0.46
TMAO	0.05

2.9 Data reporting and statistical handling

In order to relate potential methane production to methylated compound content in the initial tissue sample, total methane production in the slurries was calculated using Henry's law and the headspace methane concentration at 460 hours for seaweeds and 180 hours for coastal plants (final time point), and divided by the dry weight (calculated from moisture content) of added biomass in each slurry. Concentration of osmolytes from metabolomic analysis was also normalised to the biomass dry weight.

Separate simple linear regressions were conducted for TMA, TMAO, DMSP, choline, and sum of all methyl groups against the amount of methane produced in each slurry. The sum of methyl groups was calculated by multiplying the analysed concentration of each osmolyte by the number of methyl groups available to methanogens (TMA, TMAO, choline = 3 methyl groups, DMSP = 2 methyl groups) multiplied by the expected stoichiometry of ¾ methane molecules per methyl group (Ferry, 1999). All analyses were performed using the lm() function in R (version 4.6.0). Model fit was assessed using adjusted R^2 values, and the statistical significance of predictor variables was evaluated at $\alpha = 0.05$.

https://doi.org/10.5194/egusphere-2026-7065
Preprint. Discussion started: 26 November 2026
© Author(s) 2026. CC BY 4.0 License.

3 Results

3.1 Pure-substrate experiments and osmolyte content

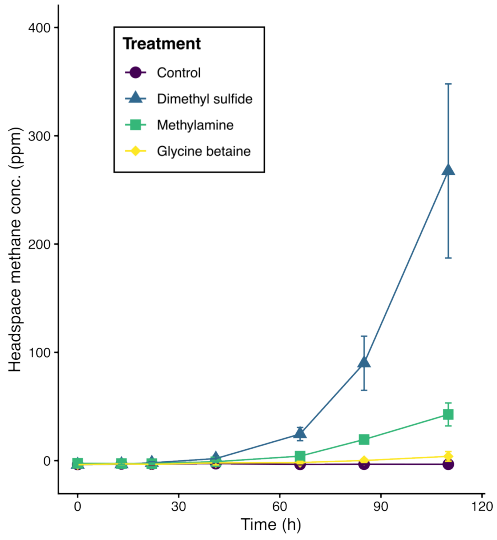


Figure 2. Pure-substrate slurries of sediment and seawater from Werribee. Concentration of all substrates was 100 µM, 'control' indicates sand and sediment without addition of any substrate. Error bars indicate standard deviation from the mean, n = 3.

Preliminary experiments showed that DMS and methylamine led to an increase in methane after approximately 60 hours of incubation, while glycine betaine stimulated negligible methane production in comparison (Fig. 2). Osmolyte concentration and composition were highly varied among the plants and seaweeds (Fig. 3). Ulva had the highest total concentrations of osmolytes, which was dominated by DMSP (100 ± 20 nmol/$mg_{tissue\ dry\ weight}$). Red filamentous algae and kelp had much lower osmolyte concentrations (< 5 nmol/$mg_{tissue\ dry\ weight}$ for any osmolyte) and were also dominated by DMSP, but a higher proportion of TMA (~20%). Coastal plants had total osmolyte concentrations in the range 4 – 10 nmol/$mg_{tissue\ dry\ weight}$ and these were dominated by choline and TMA.

https://doi.org/10.5194/egusphere-2026-7065
Preprint. Discussion started: 26 November 2026
© Author(s) 2026. CC BY 4.0 License.

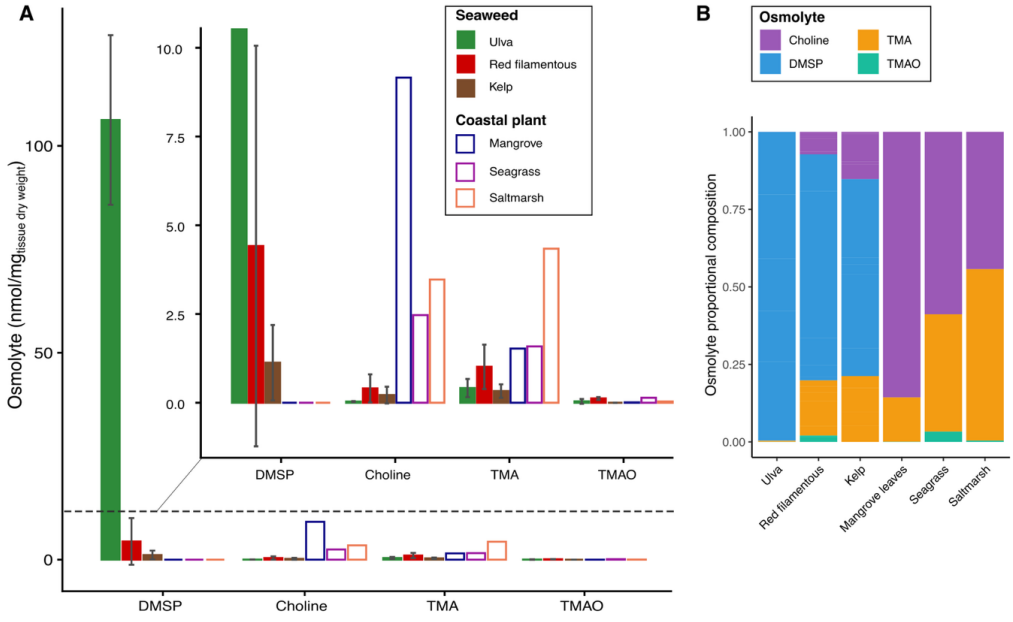


Figure 3. (A) Osmolyte content of seaweeds from different sites (filled bars, n = 5, error bars represent standard deviation) and coastal plants (empty bars, n = 1). (B) Osmolyte proportional composition of seaweeds and coastal plants

3.2 Methane production from seaweeds and coastal plants

Among seaweeds, *Ulva* stimulated the most methane production in slurries, followed by red filamentous algae, and then kelp. (1200 ± 300, 200 ± 200, 100 ± 30, and 5 ± 2 ppm at 460 hours respectively, Fig. 4A). Among coastal plants, mangrove leaves stimulated the most methane production in slurries, followed by seagrass, and then saltmarsh (5500 ± 200, 1000 ± 100, 400 ± 300, and 3 ± 4 ppm at 180 hours respectively, Fig. 4B). DMS and TMA controls showed methane production, however only to approximately 20% of their theoretical methane production potential assuming ¾ of the methyl groups present produce methane (Ferry, 1999).

https://doi.org/10.5194/egusphere-2026-7065
Preprint. Discussion started: 26 November 2026
© Author(s) 2026. CC BY 4.0 License.

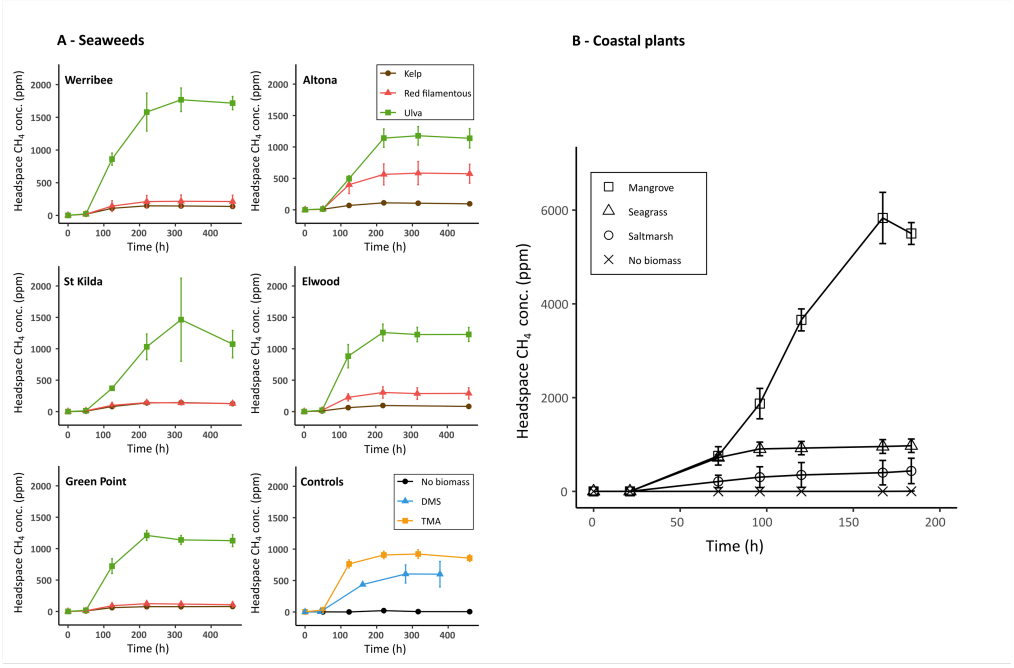


Figure 4. (A – Seaweeds) Methane production from kelp, red filamentous and Ulva seaweed species in sand slurries from five sites around Port Phillip Bay. Seaweeds were collected locally at each site. "Controls" plot shows slurry with sand only (no added biomass), or pure DMS (dimethylsulfide) or TMA (trimethylamine) 100 µM addition. Error bars represent standard deviations from triplicate slurries. (B – Coastal plants) Methane production from coastal plants in sand slurries. Error bars represent standard deviations from triplicate slurries.

3.3 Relationship between osmolyte content and methane production

When we related osmolyte content and methane production, DMSP content correlated strongly with methane production (adj. $R^2 = 0.81$, $p < 0.001$), and was the dominant component of the sum of methyl groups which stoichiometrically explained the total methane production, indicating that close to ¾ of methyl groups were converted to methane, the maximum predicted stoichiometric conversion (adj. $R^2 = 0.82$, $p < 0.001$, Fig. 5A) (Ferry, 1999).

https://doi.org/10.5194/egusphere-2026-7065
Preprint. Discussion started: 26 November 2026
© Author(s) 2026. CC BY 4.0 License.

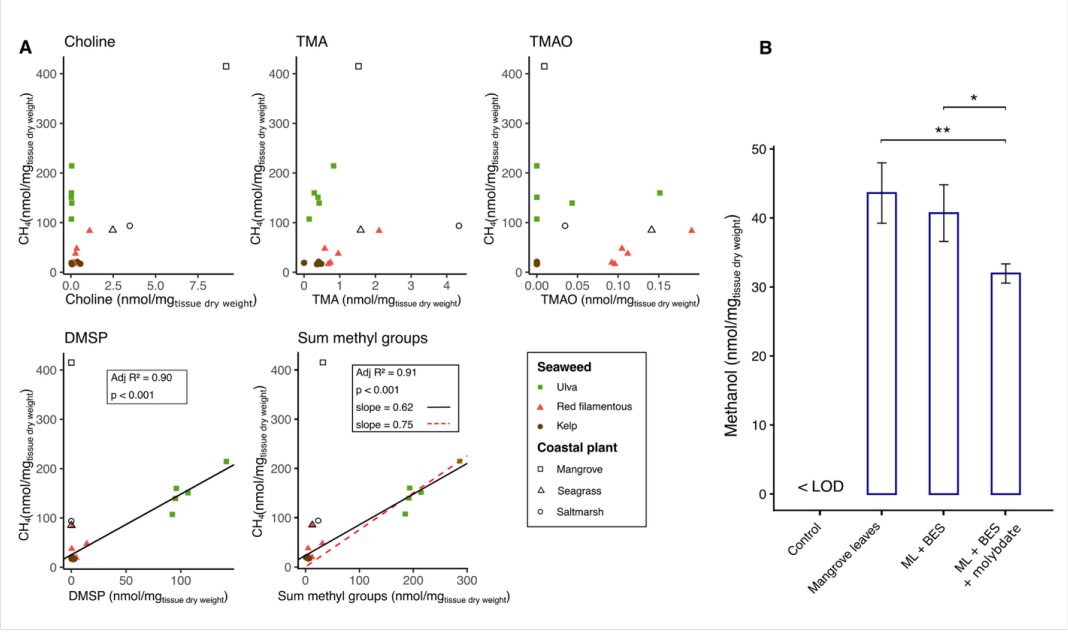


Figure 5. (A) Regression analysis of total methane production and osmolyte content of seaweeds normalised by seaweed dry mass. Regression line only shown when significance p < 0.05. Coastal plants also shown on plot but not included in regression. "Sum methyl groups" takes the sum of concentration of DMSP (dimethyl sulfoniopropionate, 2 methyl groups), TMA (trimethylamine, 3 m. g.), TMAO (trimethylamine N-oxide, 3 m. g.), and choline (3 m. g.), multiplied by the number of methyl groups available to methanogens. Red dashed line represents 3:4 line, representing the theoretical methane production from analysed osmolytes. (B) Methanol production by mangrove leaves at 144 hours with and without inhibitors of methanogenesis (BES) and sulfate reduction (molybdate). Control = sediment only. N = 3, error bars represent standard deviation. * shows pairwise comparisons where p < 0.05 and ** shows p < 0.01 (ANOVA and post-hoc Tukey HSD test).

3.4 Methanol production during mangrove leaf degradation

Despite mangrove leaves stimulating highest methane production in slurries (Fig. 4B), sum methyl groups from analysed osmolytes accounted for < 10% of methane production (32 nmol/$mg_{tissue\ dry\ weight}$, Fig. 5A). No methanol was detected in leaf extracts of fresh leaves (data not shown), however, methanol was produced in slurries at a concentration of 44 ± 4 nmol/$mg_{tissue\ dry\ weight}$ at 144 hours (Fig 5B). The addition of the methanogenesis inhibitor BES did not significantly change the methanol concentration ($p_{adj.}$= 0.67), however the addition of the sulfate reduction inhibitor, molybdate, led to significantly lower concentrations of methanol compared to mangrove leaves only ($p_{adj.}$= 0.007) and compared to mangrove leaves with BES ($p_{adj.}$= 0.033). Methanol therefore did not accumulate when methanogenesis was inhibited, and the lower methanol concentrations in the presence of molybdate could reflect either reduced methanol production or increased methanol consumption. These data alone do not show whether methanol was used for methanogenesis. No methanol was detected in the sediment only control (Fig. 5B).

https://doi.org/10.5194/egusphere-2026-7065
Preprint. Discussion started: 26 November 2026
© Author(s) 2026. CC BY 4.0 License.

3.5 Methane and methanol production in pectin and methanol amendment experiments

Methane production in unamended controls was negligible at all four sites (≤ 1.1 nmol g^{-1} after 21 days; calculated from the data in Fig. 6), and methanol in the controls remained at background concentrations (9–10 µM), apart from single replicates at Werribee South (day 3) and Wyndham Harbour (day 6). Methanol added at the start of the incubation (55–62 µM at St Kilda, Wyndham Harbour and Werribee South, and 155 µM at Patterson River) was depleted to background concentrations within 3 days at all sites (Fig. 6b, d, f, h). Methane production in the methanol treatment reached 3.1–30 nmol g^{-1} (calculated from the data in Fig. 6), equivalent to only 0.8–7.5% of the theoretical yield from the methanol consumed (Table 3).

Both pectins produced a transient increase in methanol at all sites (Fig. 6). At St Kilda, which was sampled daily, methanol peaked at 30–32 µM after 1 day and returned to background by day 4. At the other sites, methanol was 11–27 µM at the first sampling (day 3) and had returned to background by day 6 (except HM pectin at Werribee South, 15 ± 7 µM on day 6), so peak concentrations there may have been missed. At its maximum, the methanol in excess of the controls (≤ 2.2 µmol per vial) was equivalent to less than approximately 20% of the estimated methyl ester content of the pectin added. Glucose also produced a smaller transient increase in methanol (12–16 µM).

Methane production from HM pectin began after a lag of 3–6 days and after 21 days reached 263 ± 29 nmol g^{-1} at Patterson River, 111 ± 7 nmol g^{-1} at Werribee South and 105 ± 157 nmol g^{-1} at Wyndham Harbour, where one of the three replicates accounted for most of the methane (calculated from the data in Fig. 6). LM pectin produced 6- to 32-fold less methane at these sites (3.3–18.7 nmol g^{-1}). At St Kilda, both pectins produced similar, small amounts of methane (9.7 ± 10.6 and 8.0 ± 0.7 nmol g^{-1} for HM and LM pectin, respectively). Relative to the estimated methyl ester content, HM pectin yielded 8–36% of the theoretical methane at Patterson River, Wyndham Harbour and Werribee South, and LM pectin 0.4–6.3% (Table 3). HM pectin therefore produced 4- to 37-fold more methane than the methanol amendment at these three sites, although the methanol added (4.6–14.5 µmol per vial) was of a similar order to the estimated methyl ester content of HM pectin (9.7–17.1 µmol per vial). Glucose produced little methane (1.2–6.9 nmol g^{-1}; ≤ 0.02% of the theoretical yield).

Table 3. Mass balance of methane production in the amendment experiments (Sect. 2.5). Net CH_4 is the maximum mean methane production in excess of the unamended control over 21 days (n = 3), corrected for headspace sampling. Theoretical CH_4 assumes ¾ mol CH_4 per mol of methanol or pectin methyl ester and 3 mol CH_4 per mol of glucose. Methanol added is the measured initial concentration minus that in the controls. Pectin methyl ester contents are estimates (Sect. 2.5), so pectin yields are given as ranges.

Site	Amendment	Substrate added (µmol $vial^{-1}$)	Theoretical CH_4 (µmol $vial^{-1}$)	Net CH_4 (µmol $vial^{-1}$)	Yield (%)
St Kilda	Methanol	5.1	3.8	0.068	1.8
	HM pectin	9.7–17.1	7.3–12.8	0.095	0.7–1.3
	LM pectin	4.5–10.5	3.4–7.9	0.078	1.0–2.3
	Glucose	100	300	0.031	0.01
Patterson River	Methanol	14.5	10.8	0.291	2.7
	HM pectin	9.7–17.1	7.3–12.8	2.616	20–36
	LM pectin	4.5–10.5	3.4–7.9	0.113	1.4–3.3

https://doi.org/10.5194/egusphere-2026-7065
Preprint. Discussion started: 26 November 2026
© Author(s) 2026. CC BY 4.0 License.

	Glucose	100	300	0.012	< 0.01
Wyndham Harbour	Methanol	4.6	3.4	0.029	0.8
	HM pectin	9.7–17.1	7.3–12.8	1.049	8–14
	LM pectin	4.5–10.5	3.4–7.9	0.031	0.4–0.9
	Glucose	100	300	0.009	< 0.01
Werribee South	Methanol	5.2	3.9	0.289	7.5
	HM pectin	9.7–17.1	7.3–12.8	1.245	10–17
	LM pectin	4.5–10.5	3.4–7.9	0.214	2.7–6.3
	Glucose	100	300	0.060	0.02

https://doi.org/10.5194/egusphere-2026-7065
Preprint. Discussion started: 26 November 2026
© Author(s) 2026. CC BY 4.0 License.

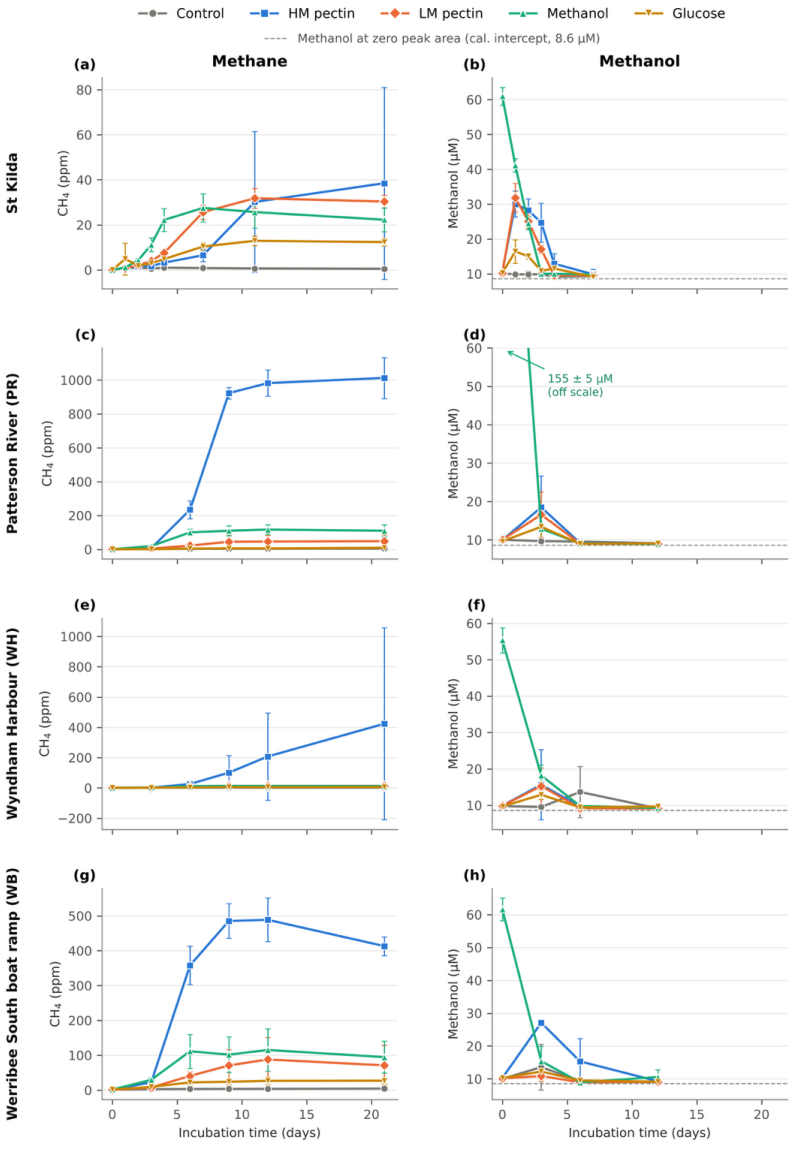


Figure 6. Headspace methane concentration (a, c, e, g) and methanol concentration (b, d, f, h) in sediment slurries from St Kilda, Patterson River, Wyndham Harbour and Werribee South, either unamended (control) or amended with high-methoxyl (HM) pectin, low-methoxyl (LM) pectin, methanol or glucose. Methane is shown as headspace concentration (ppm), as in Fig. 4. The dashed line in the methanol panels shows the concentration corresponding to zero peak area in the calibration (8.6 µM). At Patterson River, the initial methanol concentration in the methanol treatment (155 ± 5 µM) is off scale. Error bars show standard deviation (n = 3).

https://doi.org/10.5194/egusphere-2026-7065
Preprint. Discussion started: 26 November 2026
© Author(s) 2026. CC BY 4.0 License.

4 Discussion

4.1 Seaweed osmolyte content is strongly related to methane production potential

Recent work clearly shows the importance of seaweeds in methane production in seaweed farms, seaweed beds, seagrass beds and seaweed wrack (Björk et al., 2023; Roth et al., 2023; Lanari et al., 2024; Dai et al., 2025; Deng et al., 2026). Emerging evidence points to methylotrophic methane production from osmolytes as a key driver for this (Schorn et al., 2022; Hall et al., 2025), yet few studies have quantitatively linked the methane production potential of plant and seaweed biomass to its osmolyte content. Our results show that the methane production potential of seaweed is closely related to osmolyte concentration, and that DMSP, the dominant osmolyte in all three seaweeds (Fig. 3), was the main methane precursor (Fig. 5A). DMSP has been previously shown to degrade to methane (Tsola et al., 2021) and this work shows that this occurs close to the expected stoichiometry (¾ methane molecules per methyl group) under anoxic conditions. In contrast, the DMS and TMA controls produced only approximately 20% of the expected methane (Fig. 4A). We cannot explain this difference with the available data. Possible explanations include limitation by phosphorus or trace elements, which would have been supplied by the biomass in the amended slurries (Thingstad et al., 1998), consumption of DMS and TMA by non-methanogenic microorganisms, or anaerobic oxidation of part of the methane produced; we did not measure nutrients, competing pathways or methane oxidation in these slurries. Therefore, methylated osmolytes, and in particular DMSP, can give a relatively simple measure of methane production potential in seaweeds.

Although DMSP dominated the osmolyte pool of the seaweeds, methylamines may also be important methane precursors. TMA and TMAO made up approximately 20% of the osmolytes in red filamentous algae and kelp (Fig. 3B), and TMA added at 100 µM produced methane concentrations comparable to those in *Ulva* slurries (Fig. 4A). TMAO can be reduced to TMA by marine bacteria, and methylamines are non-competitive substrates for methylotrophic methanogens in sulfate-rich sediments (Oremland and Polcin, 1982; King et al., 1983). Neither TMA nor TMAO content was significantly related to methane production across the seaweeds (Fig. 5A), but their concentrations varied over a narrow range, so their contribution could not be resolved here.

The amount of methane produced in situ will depend on the proportion of biomass that decays under anoxic conditions. Our slurry incubations maximise this proportion, so the values reported here should be regarded as production potentials rather than in situ rates. Methane production in the seaweed slurries plateaued after 168–240 h (Fig. 4A). Plateaus are common in closed batch incubations, where they can result from the exhaustion of substrates or other resources. Nevertheless, the agreement between cumulative methane production and the methane expected from the measured osmolytes (Fig. 5A) suggests that osmolytes, rather than carbohydrates and proteins, were the main methane precursors in the seaweed slurries over the incubation period. We cannot exclude a contribution from other biomass components, but these require hydrolysis and fermentation before their products become available to methanogens, and the resulting acetate and hydrogen are largely consumed by sulfate reducers in marine sediments (Oremland and Polcin, 1982). Methane was detectable but low at the first time points and increased markedly over the first 120 h (Fig. 4A). This lag may reflect growth from a small seed population of methanogens (Hall et al., 2025), or an initial

https://doi.org/10.5194/egusphere-2026-7065
Preprint. Discussion started: 26 November 2026
© Author(s) 2026. CC BY 4.0 License.

period in which methane production was largely balanced by anaerobic oxidation of methane, which was not measured here.

4.2 Changing seaweed growth patterns has consequences for coastal methane emissions

The distinct methane production potential observed across seaweed taxa—and its strong positive coupling with tissue osmolyte content (Fig. 5) —takes on critical biogeochemical significance when evaluated against shifting global algal distributions. Our data show that high-osmolyte, opportunistic macroalgae have a substantially higher methane production potential than low-potential, structural brown seaweeds such as kelp. This biochemical disparity is particularly acute under climate change and coastal eutrophication scenarios, where global pressures—specifically ocean warming, marine heatwaves, and elevated agricultural and urban nutrient runoff—are rapidly altering benthic community structures (Smale, 2020; Green-Gavrielidis and Thornber, 2022; Qi et al., 2025). While thermally sensitive kelp forests are undergoing severe climate-driven declines globally (Smale and King, 2024; Smale, 2020), opportunistic green macroalgae (*Ulva* spp.) are producing larger, more frequent "green tides" fueled by rising sea temperatures and excessive nutrient loads (Xing et al., 2015; Cai et al., 2023; Green-Gavrielidis and Thornber, 2022; Qi et al., 2025). Similarly, opportunistic red filamentous algae (e.g., *Polysiphonia* and *Ceramium*) regularly form dense shoreline biomass accumulations (Eklund et al., 2005), although these occurrences remain less widespread than *Ulva* blooms (Joniver et al., 2021).

As kelp habitats decline and opportunistic algae become more abundant, the deposition of labile, osmolyte-rich biomass in shallow coastal waters is likely to increase the methane production potential of coastal sediments, particularly where decaying algal mats induce sediment and bottom-water hypoxia (Valiela et al., 1997). Whether this translates into greater emissions to the atmosphere will depend on the efficiency of aerobic and anaerobic methane oxidation in sediments and bottom waters (Mao et al., 2022; Żygadłowska et al., 2024), which we did not measure.

4.3 Non-osmolyte sources of methane from coastal plants

In contrast to the seaweeds, methylated osmolytes accounted for less than 10% of the methane produced from mangrove leaves (Fig. 5A), indicating that other precursors supported most of the methane production from this tissue. Methanol was not detected in extracts of fresh leaves, but it was present in slurries containing leaves after 144 h and absent from sediment-only controls (Fig. 5B), showing that methanol was released during leaf degradation. Pectin, a major polysaccharide of plant cell walls, contains methyl ester groups that are hydrolysed to methanol by bacterial and fungal pectin methylesterases during tissue breakdown (Chamier and Dixon, 1982; Fall and Benson, 1996; Ohimain, 2016), and the microbial demethoxylation of lignin is another possible source (Liu et al., 2025). We did not measure pectin or lignin in the leaves, however, so the source of the methanol in the mangrove slurries remains unknown.

https://doi.org/10.5194/egusphere-2026-7065
Preprint. Discussion started: 26 November 2026
© Author(s) 2026. CC BY 4.0 License.

Methanol is a well-established substrate for methylotrophic methanogens in marine and estuarine sediments (Oremland and Polcin, 1982; King et al., 1983; Zhuang et al., 2018), but our mangrove experiment does not establish that methanol fuelled the methane produced from mangrove leaves. If methanol were a major methanogenic substrate, inhibiting methanogenesis with BES would be expected to cause methanol to accumulate, and this was not observed (Fig. 5B). The absence of accumulation may be because other microorganisms, including sulfate reducers, consume methanol in these sediments (Fischer et al., 2021), but it is equally consistent with methanogens not using methanol. The BES concentration we used (30 mM) is close to the 40 mM found to be optimal for selectively inhibiting methanogens in anaerobic leach-bed systems (Kosse et al., 2016), although BES may not fully inhibit all methanogens. Because methane was not measured in these vials, the extent of inhibition could not be confirmed. Likewise, the lower methanol concentration in the presence of molybdate may reflect increased methanol consumption by methanogens once sulfate reduction was inhibited, or non-specific effects of molybdate on the fermentative bacteria that release methanol (Zane et al., 2020).

To test directly whether pectin can supply methyl groups for methanogenesis in coastal sediments, we incubated sediments from four sites with pectins of differing degrees of methyl esterification (Sect. 2.5). Both pectins released methanol within 1–3 days, showing that pectin degradation in these sediments generates a transient pool of free methanol (Fig. 6). HM pectin stimulated substantially more methane than LM pectin in three of the four sediments, consistent with the methyl ester groups of pectin being a methane precursor. In contrast, methanol added directly was depleted within 3 days, but only 0.8–7.5% of it was recovered as methane (Table 3). This indicates that most of the free methanol in these sediments was consumed by non-methanogenic pathways, such as sulfate reduction (Fischer et al., 2021). Methane production from HM pectin was 4- to 37-fold greater than from the methanol addition at three sites, even though the amount of methanol added was of a similar order to the estimated methyl ester content of the pectin, and it occurred mainly after the transient methanol pool had been depleted (Fig. 6). These observations suggest that the methyl groups of pectin may have reached methanogens without passing through the bulk methanol pool, for example through close coupling between pectin-degrading bacteria and methylotrophic methanogens, or through direct demethylation by methanogens, as reported for methoxylated aromatic compounds (Mayumi et al., 2016). Alternatively, HM and LM pectin may differ in properties other than methyl esterification, such as solubility or neutral sugar content, that affect their degradation. These experiments used different sediments from the mangrove experiment and did not include mangrove leaves, so whether pectin accounts for the methane produced from mangrove leaves remains to be tested.

4.4 High methane production potential from mangroves

Of all the seaweeds and coastal plants evaluated in this study, mangroves exhibited the highest methane production potential by a factor of two (Figs. 4 and 5A). While mangrove ecosystems are recognized for their blue carbon sequestration capacity (Macreadie et al., 2021), recent studies show that high sediment methane emissions often offset a substantial fraction of this net carbon sink (Kristensen et al., 2025; Qin et al., 2025). Environmental variables such as salinity and tidal flushing are known to modulate these fluxes (Nazareth and Gonsalves, 2022), and

https://doi.org/10.5194/egusphere-2026-7065
Preprint. Discussion started: 26 November 2026
© Author(s) 2026. CC BY 4.0 License.

sediment metagenomic surveys frequently reveal a high abundance of methylotrophic methanogens (Zhang et al., 2020). However, the specific organic precursors fueling methylotrophic activity in mangrove sediments have remained poorly defined. Our results show that methane production from mangrove leaves is not explained by their soluble osmolyte content, and our pectin experiments identify methyl-esterified cell wall polymers as one candidate source. If confirmed, the release of methyl groups from plant structural polymers during decay could help explain why mangrove sediments are methane hotspots despite high sulfate concentrations, but this hypothesis requires direct testing.

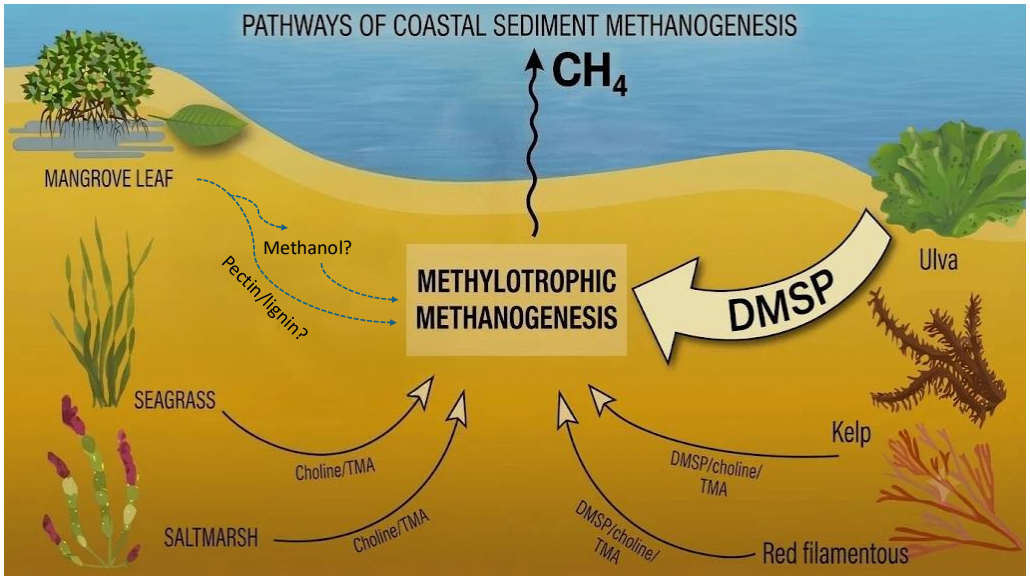


Figure 7. Conceptual model of pathways supplying methylotrophic substrates from plant and seaweed biomass in shallow marine sediments. Arrows show pathways including the release of nitrogen- and sulfur-based osmolytes (TMA = trimethylamine, TMAO = trimethylamine N-oxide, DMSP = dimethylsulfoniopropionate) on cell breakdown, with arrow width scaled to the measured osmolyte content of each type of biomass. Also shown are the hypothesised pathways (as dashed lines) of methane production by mangrove leaves from methoxy containing compounds such as pectin and lignin, possibly via methanol, or direct demethylation.

5. Conclusion and Future Outlook

This study shows that biomass-stimulated methane emissions from coastal sediments are strongly governed by species-specific biochemical profiles, revealing fundamental differences between seaweeds and vascular coastal plants. In seaweeds, methane production is tightly coupled to methylated osmolyte content (mostly DMSP), providing a direct predictive trait for assessing methanogenic potential across macroalgal functional groups. In

https://doi.org/10.5194/egusphere-2026-7065
Preprint. Discussion started: 26 November 2026
© Author(s) 2026. CC BY 4.0 License.

contrast, mangrove leaves stimulated high methane production that could not be explained by their soluble osmolyte content. Methanol was released during the degradation of both mangrove leaves and pectin, and high-methoxyl pectin stimulated more methane than low-methoxyl pectin, identifying methyl-esterified cell wall polymers as a candidate methane source. However, methanol added to the sediments was largely consumed without producing methane, so the pathway by which these methyl groups reach methanogens, and their contribution to methane production from mangrove leaves, remain to be established.

These insights highlight several critical directions for future research at the intersection of marine biogeochemistry and coastal management. First, the methyl ester content of coastal plant tissues and the fate of pectin- and lignin-derived methyl groups should be quantified, for example using ^{13}C-labelled substrates, to establish whether and how they supply methylotrophic methanogens. Second, further work must evaluate how the intense biological oxygen demand generated during macroalgal and vascular plant decay impacts microbial methane sinks. Specifically, quantifying the degree to which benthic hypoxia suppresses aerobic methane oxidation and overwhelms subsurface anaerobic oxidation will be essential for accurately forecasting net sea-to-air fluxes. Finally, as global change accelerates community regime shifts, such as the widespread loss of kelp forests to opportunistic green tides or the expansion of restored mangrove ecosystems, incorporating species-specific methane potential into blue carbon accounting frameworks is vital. Biogeochemical models must integrate these organic precursor pathways to avoid overestimating carbon burial benefits and to accurately project coastal greenhouse gas feedback under future climate and eutrophication scenarios.

Author contributions

NH and PLMC contributed to the conceptualization of the study. Methodology was developed by NH, WWW, PLMC, KJJ, CKB, and RH. The investigation was carried out by NH, SGC, LM, RH, and KJJ. NH was responsible for visualization. Funding was acquired by CG, PLMC, and WWW. Project administration was managed by PLMC and CKB, with PLMC and WWW also providing supervision. NH drafted the original manuscript, and all authors—NH, PLMC, WWW, KJJ, CKB, RH, and LM—contributed to the review and editing of the final version. AI was used to refine text and generate figure 7. All ideas and content originated from the authors

Competing interests

Perran Cook declares he is a member of the editorial board of Biogeosciences

Financial support

(PLMC, CG, WWW). National Health & Medical Research Council fellowship APP1178715 (CG).

https://doi.org/10.5194/egusphere-2026-7065
Preprint. Discussion started: 26 November 2026
© Author(s) 2026. CC BY 4.0 License.

Data availability

Data are available in the Mendeley Data repository at https://data.mendeley.com/datasets/9kj6z5h39j/1 (Dataset 1. Methane data) and https://data.mendeley.com/datasets/73kfm8jcch/1 (Dataset 2. Metabolomics data) and https://data.mendeley.com/datasets/k4878xrms7/1 (Dataset 3. Pectin and methanol amendment experiments).

References

Al-Haj, A. N. and Fulweiler, R. W.: A Synthesis of Methane Emissions from Shallow Vegetated Coastal Ecosystems, Global Change Biology, 26, 2988–3005, https://doi.org/10.1111/gcb.15046, 2020.

Björk, M., Rosenqvist, G., Gröndahl, F., and Bonaglia, S.: Methane Emissions from Macrophyte Beach Wrack on Baltic Seashores, Ambio, 52, 171–181, https://doi.org/10.1007/s13280-022-01774-4, 2023.

Borges, A. V., Champenois, W., Gypens, N., Delille, B., and Harlay, J.: Massive Marine Methane Emissions from Near-Shore Shallow Coastal Areas, Scientific Reports, 6, 27908, https://doi.org/10.1038/srep27908, 2016.

Bourke, M. F., Kessler, A. J., and Cook, P. L. M.: Influence of Buried Ulva Lactuca on Denitrification in Permeable Sediments, Marine Ecology Progress Series, 498, 85–94, https://doi.org/10.3354/meps10611, 2014.

Buelow, C. A., Connolly, R. M., Turschwell, M. P., et al.: Ambitious Global Targets for Mangrove and Seagrass Recovery, Current Biology, 32, 1641–1649, https://doi.org/10.1016/j.cub.2022.02.013, 2022.

Burg, M. B. and Ferraris, J. D.: Intracellular Organic Osmolytes: Function and Regulation, The Journal of Biological Chemistry, 283, 7309–7313, https://doi.org/10.1074/jbc.R700042200, 2008.

Bussmann, I., Brix, H., Flöser, G., Ködel, U., and Fischer, P.: Detailed Patterns of Methane Distribution in the German Bight, Frontiers in Marine Science, 8, https://doi.org/10.3389/fmars.2021.728308, 2021.

Cable, J. E., Bugna, G. C., Burnett, W. C., and Chanton, J. P.: Application of 222Rn and CH4 for Assessment of Groundwater Discharge to the Coastal Ocean, Limnology and Oceanography, 41, 1347–1353, https://doi.org/10.4319/lo.1996.41.6.1347, 1996.

Cai, J., Ni, J., Chen, Z., et al.: Effects of Ocean Acidification and Eutrophication on the Growth and Photosynthetic Performances of a Green Tide Alga Ulva Prolifera, Frontiers in Marine Science, 10, https://doi.org/10.3389/fmars.2023.1145048, 2023.

Chamier, A.-C. and Dixon, P. A.: Pectinases in Leaf Degradation by Aquatic Hyphomycetes: The Enzymes and Leaf Maceration, Microbiology, 128, 2469–2483, https://doi.org/10.1099/00221287-128-10-2469, 1982.

Chen, Y.-J., Leung, P. M., Cook, P. L. M., Wong, W. W., Hutchinson, T., Eate, V., Kessler, A. J., and Greening, C.: Hydrodynamic disturbance controls microbial community assembly and biogeochemical processes in coastal sediments, The ISME Journal, 16, 750–763, https://doi.org/10.1038/s41396-021-01111-9, 2022.

Dai, G., Chen, X., Zhuang, G., et al.: High Methane Production and Emission From Tropical Seagrasses Through Methylotrophic Methanogenesis, Geophysical Research Letters, 52, e2024GL113824, https://doi.org/10.1029/2024GL113824, 2025.

https://doi.org/10.5194/egusphere-2026-7065
Preprint. Discussion started: 26 November 2026
© Author(s) 2026. CC BY 4.0 License.



Deng, Y., Guo, X., Hu, D., Luo, H., Chen, Y., and Zhu, X.: Methane Emission Intensifies the Warming Effect of Carbon Dioxide Efflux from a Subtropical Coastal Macroalgae Aquaculture Ecosystem, Limnology and Oceanography, 71, e70293, https://doi.org/10.1002/lno.70293, 2026.

Duarte, C. M., Bruhn, A., and Krause-Jensen, D.: A Seaweed Aquaculture Imperative to Meet Global Sustainability Targets, Nature Sustainability, 5, 185–193, https://doi.org/10.1038/s41893-021-00773-9, 2022.

Eklund, B., Svensson, P. A., Jonsson, C., and Malm, T.: Toxic Effects of Decomposing Red Algae on Littoral Organisms, 2005.

Fall, R. and Benson, A. A.: Leaf Methanol — the Simplest Natural Product from Plants, Trends in Plant Science, 1, 296–301, https://doi.org/10.1016/S1360-1385(96)88175-0, 1996.

Ferry, J. G.: Enzymology of one-carbon metabolism in methanogenic pathways, Fems Microbiol. Rev., 23, 13-38, 10.1111/j.1574-6976.1999.tb00390.x, 1999.

Finster, K., King, G. M., and Bak, F.: Formation of methylmercaptan and dimethylsulfide from methoxylated aromatic compounds in anoxic marine and fresh water sediments, FEMS Microbiology Letters, 74, 295-301, 10.1111/j.1574-6968.1990.tb04076.x, 1990.

Fischer, P. Q., Sánchez-Andrea, I., Stams, A. J. M., Villanueva, L., and Sousa, D. Z.: Anaerobic microbial methanol conversion in marine sediments, Environ Microbiol, 23, 1348-1362, 10.1111/1462-2920.15434, 2021.

Green-Gavrielidis, L. A. and Thornber, C. S.: Will Climate Change Enhance Algal Blooms? The Individual and Interactive Effects of Temperature and Rain on the Macroalgae Ulva, Estuaries and Coasts, 45, 1688–1700, https://doi.org/10.1007/s12237-022-01048-y, 2022.

Hall, N., Wong, W. W., Lappan, R., et al.: Coastal Methane Emissions Driven by Aerotolerant Methanogens Using Seaweed and Seagrass Metabolites, Nature Geoscience, 1–8, https://doi.org/10.1038/s41561-025-01768-3, 2025.

ICH Harmonised Tripartite Guideline: Validation of Analytical Procedures: Text and Methodology Q2(R1), 1–13, 2005.

Joniver, C. F. H., Photiades, A., Moore, P. J., Winters, A. L., Woolmer, A., and Adams, J. M. M.: The Global Problem of Nuisance Macroalgal Blooms and Pathways to Its Use in the Circular Economy, Algal Research, https://doi.org/10.1016/j.algal.2021.102407, 2021.

Kim, G. and Hwang, D.-W.: Tidal Pumping of Groundwater into the Coastal Ocean Revealed from Submarine 222Rn and CH4 Monitoring, Geophysical Research Letters, 29, https://doi.org/10.1029/2002GL015093, 2002.

King, G. M., Klug, M. J., and Lovley, D. R.: Metabolism of acetate, methanol, and methylated amines in intertidal sediments of lowes cove, maine, Appl Environ Microbiol, 45, 1848-1853, 10.1128/aem.45.6.1848-1853.1983, 1983.

Kosse, P., Lübken, M., and Wichern, M.: Selective inhibition of methanogenic archaea in leach bed systems by sodium 2-bromoethanesulfonate, Environmental Technology & Innovation, 5, 199–207, https://doi.org/10.1016/j.eti.2016.03.003, 2016.

Kristensen, E., Flindt, M. R., and Quintana, C. O.: Predicting Climate Mitigation Through Carbon Burial in Blue Carbon Ecosystems—Challenges and Pitfalls, Global Change Biology, 31, e70022, https://doi.org/10.1111/gcb.70022, 2025.

https://doi.org/10.5194/egusphere-2026-7065
Preprint. Discussion started: 26 November 2026
© Author(s) 2026. CC BY 4.0 License.



Lanari, M., Busk, T., Holmer, M., et al.: From Sink to Source: Dynamic of Greenhouse Gases Emissions from Beach Wrack Accumulations in a Temperate Coastal Bay, Science of The Total Environment, 925, 171783, https://doi.org/10.1016/j.scitotenv.2024.171783, 2024.

Liu, T., Li, L., Xue, K., Wang, X., Li, H., Wang, Y., and Dong, X.: Methane production from lignin in anoxic peatland, Nat. Geosci., 18, 877-884, 10.1038/s41561-025-01758-5, 2025.

MacLean, B., Tomazela, D. M., Shulman, N., et al.: Skyline: An Open Source Document Editor for Creating and Analyzing Targeted Proteomics Experiments, Bioinformatics, 26, 966–968, https://doi.org/10.1093/bioinformatics/btq054, 2010.

Macreadie, P. I., Costa, M. D. P., Atwood, T. B., et al.: Blue Carbon as a Natural Climate Solution, Nature Reviews Earth & Environment, 2, 826–839, https://doi.org/10.1038/s43017-021-00224-1, 2021.

Mao, S.-H., Zhang, H.-H., Zhuang, G.-C., et al.: Aerobic Oxidation of Methane Significantly Reduces Global Diffusive Methane Emissions from Shallow Marine Waters, Nature Communications, 13, 7309, https://doi.org/10.1038/s41467-022-35082-y, 2022.

May, C. D.: Industrial pectins: sources, production and applications, Carbohydrate Polymers, 12, 79–99, https://doi.org/10.1016/0144-8617(90)90105-2, 1990.

Mayumi, D., Mochimaru, H., Tamaki, H., Yamamoto, K., Yoshioka, H., Suzuki, Y., Kamagata, Y., and Sakata, S.: Methane production from coal by a single methanogen, Science, 354, 222–225, https://doi.org/10.1126/science.aaf8821, 2016.

Nazareth, D. R. and Gonsalves, M.-J.: Influence of Seasonal and Environmental Variables on the Emission of Methane from the Mangrove Sediments of Goa, Environmental Monitoring and Assessment, 194, 249, https://doi.org/10.1007/s10661-021-09734-3, 2022.

Ohimain, E. I.: Methanol Contamination in Traditionally Fermented Alcoholic Beverages: The Microbial Dimension, SpringerPlus, 5, 1607, https://doi.org/10.1186/s40064-016-3303-1, 2016.

Oremland, R. S. and Polcin, S.: Methanogenesis and sulfate reduction: competitive and noncompetitive substrates in estuarine sediments, Appl Environ Microbiol, 44, 1270-1276, 10.1128/aem.44.6.1270-1276.1982, 1982.

Oremland, R. S., Marsh, L. M., and Polcin, S.: Methane production and simultaneous sulphate reduction in anoxic, salt marsh sediments, Nature, 296, 143-145, 10.1038/296143a0, 1982.

Oren, A.: Anaerobic degradation of organic compounds at high salt concentrations, Antonie van Leeuwenhoek, 54, 267-277, 10.1007/BF00443585, 1988.

Pino, L. K., Searle, B. C., Bollinger, J. G., Nunn, B., MacLean, B., and MacCoss, M. J.: The Skyline Ecosystem: Informatics for Quantitative Mass Spectrometry Proteomics, Mass Spectrometry Reviews, 39, 229–244, https://doi.org/10.1002/mas.21540, 2020.

Qi, L., Wang, M., Barnes, B. B., et al.: Global Floating Algae Blooms Are Expanding, Nature Communications, 17, 612, https://doi.org/10.1038/s41467-025-66822-5, 2025.

Qin, G., Lu, Z., Sanders, C., et al.: Mangrove Sediment Carbon Burial Offset by Methane Emissions from Mangrove Tree Stems, Nature Geoscience, 18, 1224–1231, https://doi.org/10.1038/s41561-025-01848-4, 2025.

https://doi.org/10.5194/egusphere-2026-7065
Preprint. Discussion started: 26 November 2026
© Author(s) 2026. CC BY 4.0 License.

Rosentreter, J. A., Borges, A. V., Deemer, B. R., et al.: Half of Global Methane Emissions Come from Highly Variable Aquatic Ecosystem Sources, Nature Geoscience, 14, 225–230, https://doi.org/10.1038/s41561-021-00715-2, 2021.

Roth, F., Broman, E., Sun, X., et al.: Methane Emissions Offset Atmospheric Carbon Dioxide Uptake in Coastal Macroalgae, Mixed Vegetation and Sediment Ecosystems, Nature Communications, 14, 42, https://doi.org/10.1038/s41467-022-35673-9, 2023.

Santos, I. R., Eyre, B. D., and Huettel, M.: The Driving Forces of Porewater and Groundwater Flow in Permeable Coastal Sediments: A Review, Estuarine, Coastal and Shelf Science, 98, 1–15, https://doi.org/10.1016/j.ecss.2011.10.024, 2012.

Schorn, S., Ahmerkamp, S., Bullock, E., et al.: Diverse Methylotrophic Methanogenic Archaea Cause High Methane Emissions from Seagrass Meadows, Proceedings of the National Academy of Sciences, 119, e2106628119, https://doi.org/10.1073/pnas.2106628119, 2022.

Skyline for Small Molecules: A Unifying Software Package for Quantitative Metabolomics, Journal of Proteome Research, https://pubs.acs.org/doi/10.1021/acs.jproteome.9b00640, n.d.

Smale, D. A.: Impacts of Ocean Warming on Kelp Forest Ecosystems, New Phytologist, 225, 1447–1454, https://doi.org/10.1111/nph.16107, 2020.

Smale, D. A. and King, N. G.: Marine Macrophytes in a Changing World: Mechanisms Underpinning Responses and Resilience to Environmental Stress, New Phytologist, 244, 1675–1677, https://doi.org/10.1111/nph.20215, 2024.

Thingstad, T. F., Zweifel, U. L., and Rassoulzadegan, F.: P limitation of heterotrophic bacteria and phytoplankton in the northwest Mediterranean, Limnol. Oceanogr., 43, 88-94, https://doi.org/10.4319/lo.1998.43.1.0088, 1998.

Trégarot, E., D'Olivo, J. P., Botelho, A. Z., et al.: Effects of Climate Change on Marine Coastal Ecosystems — A Review to Guide Research and Management, Biological Conservation, 289, 110394, https://doi.org/10.1016/j.biocon.2023.110394, 2024.

Tsola, S. L., Zhu, Y., Ghurnee, O., Economou, C. K., Trimmer, M., and Eyice, Ö.: Diversity of Dimethylsulfide-Degrading Methanogens and Sulfate-Reducing Bacteria in Anoxic Sediments along the Medway Estuary, UK, Environmental Microbiology, 23, 4434–4449, https://doi.org/10.1111/1462-2920.15637, 2021.

Valero-Rodriguez, J. M., Dempster, T., Wong, W. W., Lewis, J. A., Cook, P. L. M., and Swearer, S. E.: Spatio-Temporal Patterns in the Biomass, Species Composition and Nitrogen Content of Drift Macroalgae in an Urbanised Coastal Embayment, Journal of Applied Phycology, 36, 2369–2381, https://doi.org/10.1007/s10811-024-03249-3, 2024.

Valiela, I., McClelland, J., Hauxwell, J., Behr, P. J., Hersh, D., and Foreman, K.: Macroalgal blooms in shallow estuaries: Controls and ecophysiological and ecosystem consequences, Limnol. Oceanogr., 42, 1105-1118, https://doi.org/10.4319/lo.1997.42.5_part_2.1105, 1997.

Wang, J.-J., Li, X.-Z., Lin, S.-W., and Ma, Y.-X.: Economic Evaluation and Systematic Review of Salt Marsh Restoration Projects at a Global Scale, Frontiers in Ecology and Evolution, 10, https://doi.org/10.3389/fevo.2022.865516, 2022.

Wang, M., Hu, C., Barnes, B. B., Mitchum, G., Lapointe, B., and Montoya, J. P.: The Great Atlantic Sargassum Belt, Science, 365, 83–87, https://doi.org/10.1126/science.aaw7912, 2019.

https://doi.org/10.5194/egusphere-2026-7065
Preprint. Discussion started: 26 November 2026
© Author(s) 2026. CC BY 4.0 License.

Wang, Q., Alowaifeer, A., Kerner, P., et al.: Aerobic Bacterial Methane Synthesis, Proceedings of the National Academy of Sciences, 118, e2019229118, https://doi.org/10.1073/pnas.2019229118, 2021.

Wang, X.-C. and Lee, C.: Sources and distribution of aliphatic amines in salt marsh sediment, Org. Geochem., 22, 1005-1021, https://doi.org/10.1016/0146-6380(94)90034-5, 1994.

Weber, T., Wiseman, N. A., and Kock, A.: Global Ocean Methane Emissions Dominated by Shallow Coastal Waters, Nature Communications, 10, 4584, https://doi.org/10.1038/s41467-019-12541-7, 2019.

Wiesenburg, D. A. and Guinasso, N. L.: Equilibrium solubilities of methane, carbon monoxide, and hydrogen in water and sea water, Journal of Chemical & Engineering Data, 24, 356–360, https://doi.org/10.1021/je60083a006, 1979.

Wong, W. W., Cartwright, I., Poh, S. C., and Cook, P.: Sources and Cycling of Nitrogen Revealed by Stable Isotopes in a Highly Populated Large Temperate Coastal Embayment, Science of The Total Environment, 806, 150408, https://doi.org/10.1016/j.scitotenv.2021.150408, 2022.

Xiao, K.-Q., Beulig, F., Røy, H., Jørgensen, B. B., and Risgaard-Petersen, N.: Methylotrophic Methanogenesis Fuels Cryptic Methane Cycling in Marine Surface Sediment, Limnology and Oceanography, 63, 1519–1527, https://doi.org/10.1002/lno.10788, 2018.

Xing, Q., Tosi, L., Braga, F., Gao, X., and Gao, M.: Interpreting the Progressive Eutrophication behind the World's Largest Macroalgal Blooms with Water Quality and Ocean Color Data, Natural Hazards, 78, 7–21, https://doi.org/10.1007/s11069-015-1694-x, 2015.

Yoch, D. C.: Dimethylsulfoniopropionate: Its Sources, Role in the Marine Food Web, and Biological Degradation to Dimethylsulfide, Applied and Environmental Microbiology, 68, 5804–5815, https://doi.org/10.1128/AEM.68.12.5804-5815.2002, 2002.

Zane, G. M., Wall, J. D., and De León, K. B.: Novel Mode of Molybdate Inhibition of Desulfovibrio vulgaris Hildenborough, Frontiers in Microbiology, Volume 11 - 2020, 2020.

Zhang, C.-J., Pan, J., Liu, Y., Duan, C.-H., and Li, M.: Genomic and Transcriptomic Insights into Methanogenesis Potential of Novel Methanogens from Mangrove Sediments, Microbiome, 8, 94, https://doi.org/10.1186/s40168-020-00876-z, 2020.

Zhuang, G.-C., Heuer, V. B., Lazar, C. S., Goldhammer, T., Wendt, J., Samarkin, V. A., Elvert, M., Teske, A. P., Joye, S. B., and Hinrichs, K.-U.: Relative importance of methylotrophic methanogenesis in sediments of the Western Mediterranean Sea, Geochim. Cosmochim. Acta, 224, 171-186, https://doi.org/10.1016/j.gca.2017.12.024, 2018.

Zhuang, G.-C., Liu, Q., Yuan, L., Wu, B., Sui, X., Zhou, Z., Wang, J., Dong, L., Liu, X., Yang, G.-P., and Wang, F.: Controls and contributions of methylotrophic methanogenesis to methane production in coastal sediments, Limnol. Oceanogr., 71, e70269, https://doi.org/10.1002/lno.70269, 2026.

Żygadłowska, O. M., Roth, F., van Helmond, N. A. G. M., Lenstra, W. K., Venetz, J., Dotsios, N., Röckmann, T., Veraart, A. J., Stranne, C., Humborg, C., Jetten, M. S. M., and Slomp, C. P.: Eutrophication and Deoxygenation Drive High Methane Emissions from a Brackish Coastal System, Environmental Science & Technology, 58, 10582-10590, 10.1021/acs.est.4c00702, 2024.